Terminal-Side Interference Mitigation for Spectral Coexistence of Satellite and Terrestrial Systems in Non-Exclusive Ka-band

Shree Krishna Sharma, Symeon Chatzinotas, and Björn Ottersten
SnT - securityandtrust.lu, University of Luxembourg, Luxembourg
Contact: 4, rue Alphonse Weicker, L-2721, Ph: (+352)4666445865,
Email: {shree.sharma, symeon.chatzinotas, bjorn.ottersten}@uni.lu.

One of the promising solutions to address the spectrum scarcity problem in Satellite Communications (SatComs) is to exploit the use of non-exclusive Ka-band spectrum, which is primarily allocated to terrestrial Fixed Service (FS) microwave links. In this regard, this paper considers the spectral coexistence of FS links with the Fixed Satellite Services (FSS) system both in the downlink and the uplink. Out of several possible solutions to enable this coexistence, this paper deals with the terminal-side Sidelobe (SL) suppression and Beamforming (BF) techniques at the FSS terminal. Starting with a detailed review of existing SL suppression, BF techniques as well as Ka-band terminal status, first, we provide the detailed methodology on the employed raster scan based Direction of Arrival (DoA) estimation method. Subsequently, with the help of numerical results, we provide the performance evaluation of one SL suppression technique and one BF technique, considering a parabolic reflector with an array of auxiliary elements and the array of feeds, respectively. Finally, we discuss several interesting practical aspects to be considered while designing the proposed solutions.

***Index Terms*: Terminal-side beamforming, Satellite-terrestrial coexistence, Ka-band non-exclusive spectrum, Sidelobe suppression**

I. Introduction

The usable satellite spectrum has become scarce due to continuously increasing demand for multimedia, broadcast, and interactive services and the current static frequency allocation policies. In this context, current trend is the investigation of higher frequency bands such as Ku/Ka bands [1], and even Q/V/optical bands for the feeder links. Towards enhancing the satellite system capacity, satellite systems have already moved from a single-beam paradigm to the multibeam platform. However, there still exists a huge gap to meet the Terabit/s capacity requirement within the 2020 horizon. One promising way to solve the spectrum scarcity problem in Satellite Communication (SatCom) is to enhance the utilization of available spectrum using cognitive radio approaches such as dynamic spectrum access or spectrum sharing [2–5].

While considering the operation of Geostationary (GEO) Fixed Satellite Services (FSS) systems in the Ka-band, only 500 MHz exclusive spectrum is available in the downlink (19.7-20.2 GHz) and the same in the uplink (29.5-30 GHz). In this regard, one potential solution of enhancing the capacity of next generation of satellite systems is to utilize the non-exclusive Ka-band (2 GHz (17.7-19.7 GHz) in the forward link and 2 GHz (27.5-29.5 GHz) in the return link), which is primarily assigned to terrestrial Fixed Service (FS) microwave links. In order to exploit this non-exclusive by the FSS systems, the following two coexistence scenarios are promising: (i) coexistence of FSS downlink and FS links in 17.7-19.7 GHz, and (ii) coexistence of FSS uplink with FS links in 27.5-29.5 GHz.

In order to enable the aforementioned coexistence scenarios, several techniques such as database approach, resource allocation and interference mitigation techniques can be exploited at the FSS system [6, 7]. Although several interference mitigation techniques such as precoding, multiuser detection and Beamforming (BF) have been investigated at the gateway side, the concept of applying suitable interference mitigation techniques at the satellite terminals is relatively new [8, 9]. In this regard, the main objective of this work is to exploit suitable interference mitigation techniques at the FSS terminal considering multi-feed/element based antenna structure instead of the conventional single feed-based parabolic reflector. The Sidelobes (SLs) of an antenna configuration may cause harmful interference to the unwanted or incumbent receivers in the considered spectral coexistence scenarios, and therefore needs to be reduced below the desired limit. In this regard, suitable SL suppression techniques can be employed to reduce the radiation received from (or transmitted to) the sidelobes of an antenna. On the other hand, adaptive BF technique can be applied to maximize transmission/reception to/from the desired direction and to mitigate interference from/to interfering/victim directions.

In contrast to the widely used Uniform Linear Array (ULA) structure in the terrestrial BF literature, in this work, a parabolic reflector is used along with the auxiliary radiators and with the the array of the feeds in order to design SL suppression and BF techniques, respectively. Besides, in contrast to the widely used two dimensional (2D) BF, a three dimensional (3D) BF approach, which controls radiation pattern in both elevation and azimuth planes, is followed. Moreover, in the forward link coexistence scenario, a raster scan approach is investigated at the FSS terminal in order to estimate the Direction of Arrival (DoA) of the interfering directions in the worst case (high interference) scenario considering the FS database of Poland. Subsequently, suitable signal processing algorithms are applied in order to create nulls in these interfering directions and to maximize its transmission in the desired direction. Similarly, in the return link, sector based and blind approaches are applied in the worst case scenario considering the FS database of Slovakia.

The remainder of this paper is structured as follows: Section II describes the considered coexistence scenarios and the associated interference issues. Section III provides a detailed overview of the SL suppression, adaptive BF techniques and the status of Ka-band terminal. Section IV presents the generalized signal model while Section V illustrates the employed raster scan based DoA estimation method. Section VI presents the employed SL suppression along with some numerical examples and Section VII describes the employed BF method. Finally, Section VIII highlights several practical considerations and Section IX concludes the paper.

II. Scenarios and Problem Description

Figures 1 (a) and 1 (b) present the spectral coexistence scenario of FSS system with a terrestrial FS link in the forward link (17.7-19.7 GHz) and in the return link (27.5-29.5 GHz), respectively. In order to enable these coexistence scenarios, inter-system interference need to be handled carefully. Mainly, the following issues need to be addressed: (i) in the downlink (17.7-19.7 GHz band), FSS systems can not claim protection against other terrestrial services allocated to the same band and hence the FSS system has to protect its terminals from the harmful interference caused by the FS transmitters, and (ii) in the uplink (27.5-29.5 GHz band), FSS systems have to guarantee sufficient interference protection to the FS receivers. In this regard, how to utilize the non-exclusive Ka-band by FSS systems effectively without receiving/causing harmful interference from/to terrestrial FS systems is the main research challenge.

The main challenges in designing signal processing techniques for SL suppression and adaptive BF techniques at the FSS terminal in the considered scenarios are the following.

1. Each element in the array has a directive pattern instead of the widely used omnidirectional nature for the ULA.

2. In contrast to the case of ULA, no analytical expression for the array response vector is available and this needs to be obtained numerically.

3. Most of the BF techniques need information about the DoAs of interfering/victim stations. How to obtain this knowledge accurately and how to apply BF in the scenarios where this

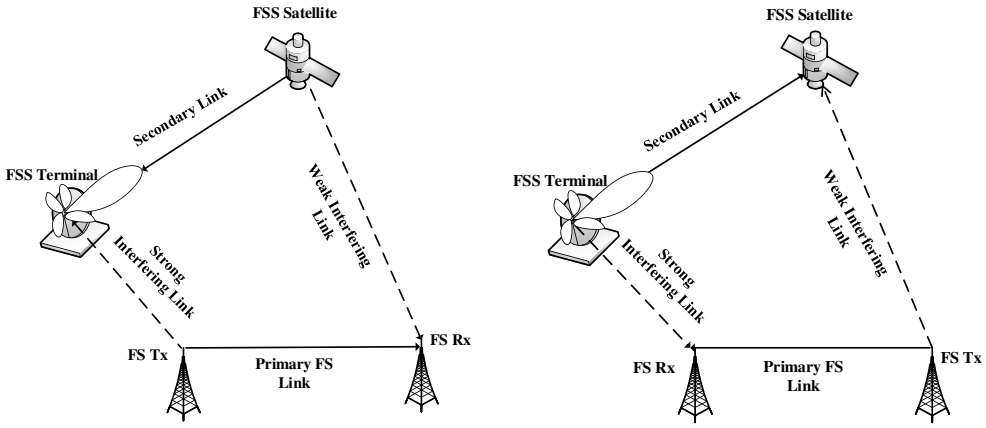

(a) (b)

Figure 1: Spectral coexistence scenario of an FS link with the FSS system in (a) forward link (17.7-19.7 GHz), (b) return link (27.5-29.5 GHz)

knowledge is not available are other important issues to be considered.

4. Due to practical cost and implementation constraints, only a few number of array elements/feeds are feasible at the FSS terminal's antenna structure. Therefore, how to handle the high number of interfering sources/victims is a challenging issue.

III. State of Art Review

In this section, we briefly review the state of art related to signal processing techniques employed for SL suppression and adaptive BF purposes. Besides guaranteeing the desired gain in the direction of interest, adaptive signal processing techniques can reject unwanted interference signals by placing nulls in the direction of the interfering/victim directions. In practical scenarios, where the directions of the interfering/victim stations are unavailable, adaptive processing can still reduce the radiated power in the undesired directions by employing suitable SL suppression mechanisms. Several parameters of the beam pattern such as peak directivity, the locations of peaks and nulls, null depth, relative SL levels, etc. can be varied by controlling the amplitudes and phases of the radio frequency signals transmitted/received from each antenna element. This control requires suitable signal processing techniques to be employed at the signal processing block of the BF circuitry.

III.A. Sidelobe suppression techniques

The effect of SLs in the spectral coexistence scenarios can be mitigated either by investigating a suitable antenna structure which produces smaller side-lobes in its radiation pattern or by using signal processing techniques which can mitigate the effect of the interference caused by the sidelobes of transmit/receive antennas. Moreover, the interference rejection at the satellite terminal's receiver can be accomplished by designing its antenna pattern in such a way that pattern minima or nulls are placed in the directions of the interfering sources. If the locations of interferers are known beforehand, then the receive antenna pattern can be designed by placing nulls in the corresponding interfering directions. However, the interference environment is varying and the antenna should be capable of adapting its pattern accordingly. Depending on whether the knowledge about the interference environment is available or not, the SL levels of the radiation pattern can be adjusted. For example, the beampattern with constant sidelobe levels usually assumes that the interference is equally likely to arrive anywhere in the SL region. If the interference environment is known, i.e., the positions of the interfering sources with respect to the transmitting antenna, then adaptive nulling can be performed towards these interfering positions

In terrestrial/satellite/radar communication systems, various techniques have been used in the past to reduce certain sidelobes and in turn the interference from the adjacent links. Figure 2 lists the available SL suppression techniques in the literature and their classifications. In the following, we provide a brief review of these SL suppression/cancellation techniques.

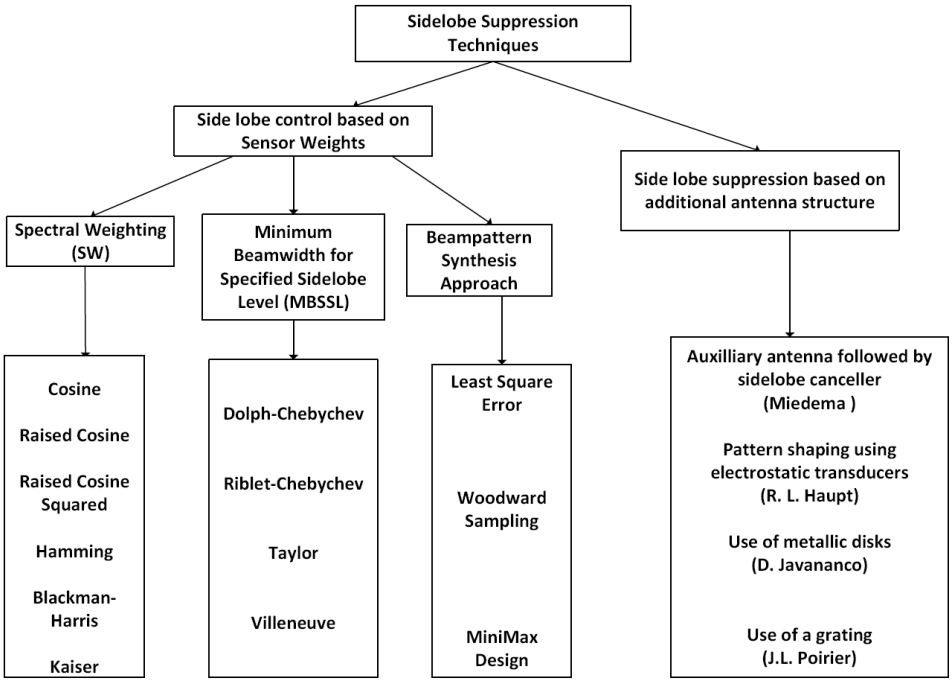

Figure 2: Classification of sidelobe suppression techniques

III.B. Sidelobe Control based on Sensor Weights

In this approach, SLs of an antenna radiation pattern are controlled by providing proper weights to the sensors of the array. These weights can be designed based on different criteria, mainly the following [10]: (i) Spectral Weighting (SW), (ii) Minimum Beamwidth for Specified Sidelobe Level (MBSSL), and (iii) Beampattern synthesis. These approaches are briefly described below.

1. Spectral Weighting (SW): This approach exploits the Fourier transform relationships between the weighting function and the frequency-wavenumber response for a linear array with a sensor spacing less than or equal to half of the wavelength (λ). Examples of the weighting windows include uniform, cosine, raised cosine, raised cosine squared, hamming, Balckman-Harris, Kaiser, etc. In this approach, the sidelobes decay asymptotically based on the order of the discontinuity in the aperture weighting.

2. Minimum Beamwidth for Specified Sidelobe Level (MBSSL): This approach attempts to find an array weighting function that minimizes the beamwidth for a given maximum sidelobe level. The following techniques exist under this category [10]: (i) Dolph-Chebychev, (ii) Riblet-Chebychev, (iii) Taylor, and (iv) Villeneuve. Depending on the employed technique, SL levels may vary across the radiation pattern, for example, constant SL levels for the Dolph-Chebychev approach and decaying Sl levels in the Taylor approach.

3. Beampattern Synthesis Approach: In this approach, the beampattern is synthesized based on a certain reference or an objective. As reflected in Fig. 2, there are the following categories under this approach: (i) Least Square Error approach, (ii) Woodward Sampling, and (iii)

MiniMax Design.

III.C. Sidelobe Control based on Additional Antenna Structure

This category of SL suppression approach is mainly investigated for a parabolic reflector, which is the widely used antenna structure for satellite terminals. In many cases, this approach requires additional structures such as auxiliary antenna/s, metallic disk/s, grating/s, and electrostatic transducers in addition to the main reflector in order to suppress the interference/transmission via sidelobes. In this direction, there exist several patents [11–15] which use different SL control approaches.

SL suppression in directional antennas is generally accomplished by combining the signal from the main antenna with that of an auxiliary antenna by applying suitable adjustments in amplitude and phase. Since the auxiliary antenna is usually much smaller than the main antenna, their radiation patterns do not match and this SL suppression approach usually becomes effective only over a narrow bandwidth and smaller angular sector. This approach can be extended to the wide bandwidth by introducing special equalizing networks, however, equalization networks increase the complexity and the cost of the system. To this end, the patent [11] proposes antenna arrangements comprising of a main antenna including a main reflector, a feed horn and auxiliary elements. Besides, the U.S. patent by W. E. Buehler *et al* [12] firstly proposed a multiple feed arrangement for microwave parabolic antennas which includes a parabolic reflector, and a plurality of individually fed illuminators.

Another approach for SL suppression is by changing a reector antenna mechanically. With this approach, it is possible to create a desired null in several ways. In [13], the actuators of an electrostatic reector antenna are adaptively adjusted to place a null in the far-eld pattern. In this method, the electrostatic transducers are used to shape the reflector and generate a vibration used to modulate the envelope of the signals received from the SLs while the signals from the main lobe remain unaltered. Subsequently, a low pass filter placed after the feed system performs the filtering of the interference signals. Besides, the contribution in patent [14] proposes a method based on the use of two or more metallic disks on the reflector surface placed at specific distances from the main reflector in order to generate a null in the direction of interest. By adjusting the spacing between the disks and the reflector surface, it is possible to vary the phase and amplitude of the resulting nulling signal. The main drawback of this technique is that it requires a manual installation of the disks and a tuning to obtain the nulls in the desired direction of the far field. Furthermore, at least two interacting disks are needed to achieve amplitude as well as phase control.

To address the aforementioned issues, the patent [15] investigates a reflector antenna having an adaptive SL nulling assembly, which comprises a disk-shaped mounting plate having a shaft aligned with the rotational axis thereof and passing through the main reflector focusing surface and is oriented to direct electromagnetic energy into the feed horn of the main antenna. In this approach, the amplitude of the signal reflected from the nulling assembly is controlled by rotating the assembly, and its phase is controlled by adjusting the spacing between the grating on the nulling assembly. The issue of multiple nulling can be addressed by using additional nulling elements in order to create nulls towards the multiple interfering sources/receivers. In addition, the contribution in [16] proposes an adaptive nulling system for cylindrical parabolic reector antennas. In this approach, the null is controlled using an adjustable scatter element and a genetic algorithm is used to mechanically adjust scattering elements in order to place nulls in the SLs of the reflector antenna. It is shown that there exists a tradeoff between size and number of scattering elements and quality of nulls and pattern distortion.

III.D. Adaptive Beamforming Techniques

Existing BF solutions can be classified on different bases as depicted in Figure 3. The detailed description on several types of beamformers on different bases as highlighted in Fig. 3 can be found in [17]. Depending on whether the combining weights are dependent on the received data or not, BF techniques can be broadly categorized into two classes: (i) Data independent (fixed) beamformers in which the weights are chosen in such a way that the beamformer's response approximates a

desired pattern independent of the array data or data statistics, (ii) Data dependent beamformers in which BF weights are chosen based on the statistics of the data received at the array. The main goal of latter category of beamformers is to optimize the beamformer's response in such a way that the output contains minimal contributions due to noise and interfering signals. Depending on the optimality of the BF design, this data dependent approach can be (i) statistically optimum, and (ii) sub-optimum. Out of these, statistically optimum beamformers can be divided into the following categories: (i) Minimum Mean Square Error (MMSE), (ii) Minimum Output Energy (MOE), and (iii) SINR Maximization.

From the practical implementation perspectives, optimal BF techniques may be difficult to implement in practice due to the absence of knowledge of the covariance matrix. In case the DoA knowledge is not available, one can investigate several iterative and non-iterative approaches such as Direct Matrix Inversion (DMI), Steepest descent, Least Mean Square (LMS) Algorithm, Recursive Least Square (RLS) Algorithm and Constant Modulus Algorithm (CMA) indicated in Fig. 3. As highlighted earlier, most of the existing BF literature in the context of SatCom focuses on the BF design either at the space side or gateway side. However, the topic of adaptive BF at the terminal side has received limited attention [8, 9, 18, 19]. The BF weights in many cases are the functions of the covariance matrices which are eventually the functions of the steering vectors in Line of Sight (LoS) channels.

Smart antennas capable of performing digital BF at Ka-band frequencies can be promising elements for future broadband SatCom systems. In this context, the contribution in [18] studies a modular receive and transmit antenna terminal featuring digital BF at Ka-band frequencies within the framework of project Smart Antenna Terminal (SANTANA). The recent contribution in [19] provides an overview of aspects encountered during the design and realization of highly integrated antenna frontends dedicated to SatCom-on-the-move.

In a DoA-based adaptive beamformer, the BF weights are designed based on the knowledge of DoA information of the desired/interfering terminals. If the DoA information of the desired and interfering terminals is not available to the beamformer beforehand, range aware adaptive BF approaches can be exploited. For example, authors in [20, 21] have studied the applications of different BF techniques such as LCMV and MVDR in the spectral coexistence scenario of satellite and terrestrial networks by using the special propagation characteristics of GEO satellite terminals. It has been shown that it is possible to create nulls over a desired area of interest by using these techniques and can be applied for both transmit and receive BF scenarios.

III.E. Ka-band Terminal Status

Reflector antenna is the most commonly used terminal antenna for Ka band SatCom systems and it is generally made of a parabolic reflector with an antenna feed. In the receive mode, the reflector focuses the incoming plane wave from a given direction to the feed and in the transmit mode, the signal radiated by the feed is converted by the reflector to a narrow beam. The beamwidth of the constructed beam depends on the reflector size (diameter) and the operating frequency. Due to antenna reciprocity principle, the beamwidth for the transmit and receive beams are same for the same reflector and feed combination and for a given frequency. Feed antennas are usually horn antennas. In particular, single horns are used to generate relatively simple circularly symmetric beams while multiple horns are used to generate shaped beams.

From the cost perspectives, conventional reflectors are preferred, however, different transmit and receive frequencies lead to the use of either a dual-frequency horn or two independent horns [23]. The main drawback with the dual-frequency horn is that the phase-centre is different at each frequency, and thus may result in the reduction of the antenna gain. The method of using independent feeds for transmit and receive purposes is simpler but its realization with reflector antennas is difficult since different positions cannot generate a beam in the same direction. In this context, authors in [23] describe the design, manufacturing and test of a printed reflect-array for Ka-band terminal antenna. The concept behind this design is that a reflect-array can be designed with two independent feeds when the transmission and the reception links are in orthogonal linear polarizations with one feed for the uplink and another for the downlink. For high-gain terminal antennas, printed reflect arrays can be of particular interest due to their low cost, ease of manufacture and reconfigurability.

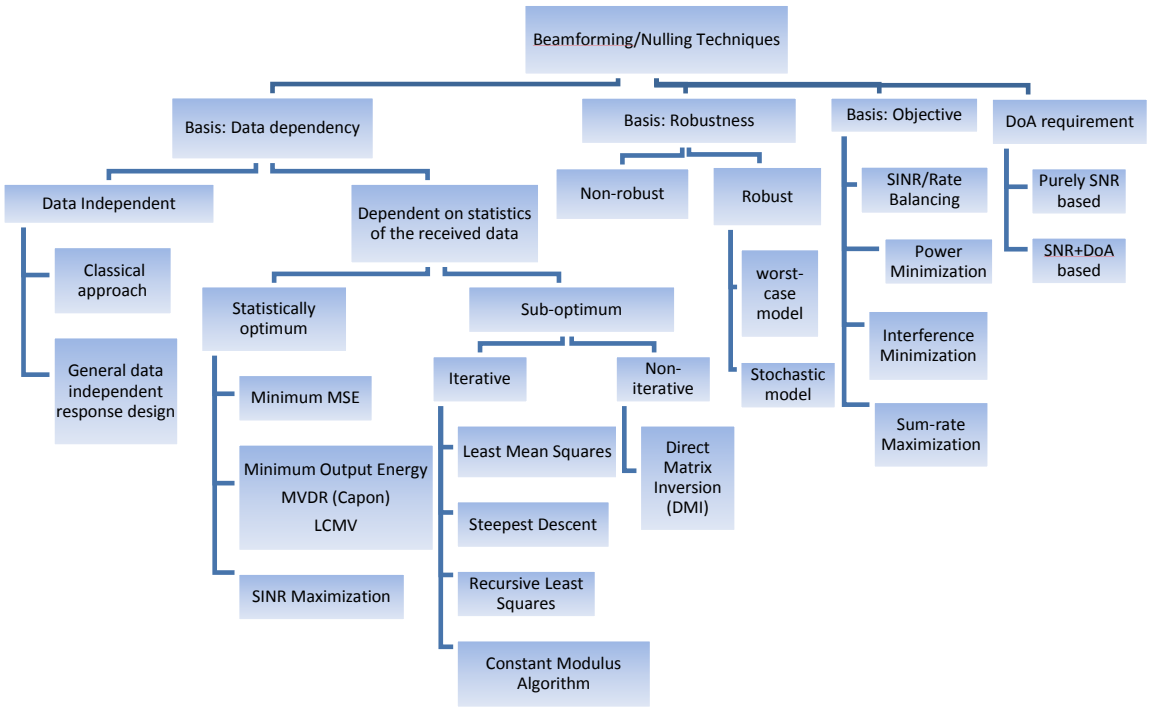

Figure 3: Classification of beamforming/nulling techniques

Recently, authors in [22] present the design and testing of a passive dual frequency printed Fresnel reflector which could be used as ground terminals for Ka-band SatCom systems. The reflect array is increasingly receiving attention in the areas of infrared and THz communications as well [24].

The currently available terminal antenna structure suitable for the BF purpose is multi-antenna satellite receiver dish which may consist of multiple feeds, with several low noise block convertors (LNBs), called Multiple LNB (MLNB) structure. In practice, the number of LNBs should be kept low e.g., 2-3 LNBs, due to cost, mechanical support and electromagnetic blockage issues [25]. It can be noted that in the presence of multiple harmful FS links, the considered scenario becomes overloaded since the satellite receiver usually has fewer LNBs than the received co-channel FS signals. In this context, a receiver structure with an arbitrary number of LNBs has been proposed in [25] for broadcast reception under interference environment generated by adjacent satellites. Similar concept can be applied in order to improve the detection of DVB-S2 signal reception in the presence of multiple harmful FS interfering users. The main difference in the considered scenario from the overloaded scenario considered in [25] is that the harmful FS interference can enter to the satellite terminal from any direction instead of the main lobe. Since it is not feasible to place a large number of antennas at the satellite terminal due to cost and implementation aspects, the number of nulls that can be created are limited. However, in the regions where sparse FS microwave links are present, the satellite terminal may not need to protect a large number of incumbent FS transmitters within its coverage region.

IV. Signal Model

The FSS terminal can be assumed to be equipped with a suitable array antenna or array fed reflector. In this regard, European Space Agency (ESA) project ASPIM has identified the following antenna structures [26]: (i) array of auxiliary elements placed on the top of the main reflector rim, (ii) Feed Array Reflector (FAR), and (iii) Direct-radiating array. Out of these, the first structure was used for SL suppression purpose whereas the other two for the BF purpose.

For our analysis, a narrow-band plane wave impinging on the considered antenna structure

from the far-field region is considered. For the generalized signal model, we consider N number of feeds/elements in the antenna structure, one desired direction towards the FSS satellite and K number of interfering FS stations. Let (θ_0, ϕ_0) denote the 2D angular position of the desired FSS satellite and (θ_k, ϕ_k), $k \in \{k = 1, ..., K\}$, denotes the 2D location of the kth interfering station. Then, the $N \times 1$ received signal vector $\mathbf{y}$ at the FSS terminal can be written as

$$\mathbf{y} = h_0 \mathbf{a}(\theta_0, \phi_0) s_0 + \sum_{k=1}^{K} h_k \mathbf{a}(\theta_k, \phi_k) s_k + \mathbf{z}, \tag{1}$$

where s_0 is the transmitted FSS signal, s_k is the transmitted signal from the kth interfering FS station, $\mathbf{z}$ denotes the $N \times 1$ Additive White Gaussian Noise (AWGN) vector, $\mathbf{a}(\theta_0, \phi_0)$ denotes the antenna response vector in the desired direction (θ_0, ϕ_0) while $\mathbf{a}(\theta_k, \phi_k)$ denotes the antenna response vector towards the kth interfering FS station, h_k represents the channel gain of the link towards the kth interfering station and it is assumed to be constant for all the antenna elements. The array response vector $\mathbf{a}(\theta, \phi)$ in the (θ, ϕ) can be written as

$$\mathbf{a}(\theta, \phi) = [c_1 e^{j\Psi_1}, c_2 e^{j\Psi_2}, \ldots, c_N e^{j\Psi_N}]^T, \tag{2}$$

where c_i and Ψ_i denote the amplitude gain and the phase of the ith feed $(i = 1, \ldots, N)$ to a unit amplitude plane wave coming from the direction (θ, ϕ), respectively. For the considered antenna structures, the response vector can be calculated based on the amplitude and phase values at each individual feeds using the software GRASP, which is widely used tool for the design of parabolic reflectors [27].

After evaluating the weighting coefficients using a suitable SL or BF technique, the received signal vector $\mathbf{y}$ in (1) is then linearly combined through an $N \times 1$ complex weight vector $\mathbf{w}$ to yield the output y_1 in the following way; $y_1 = \mathbf{w}^\dagger \mathbf{y}$, where $(\cdot)^\dagger$ denotes the Hermitian transpose.

V. Direction of Arrival (DoA) Estimation

The DoAs of interfering/victim stations should be known to apply many BF algorithms. The acquisition of Channel State Information (CSI) as well as the DoA information at the transmit side for transmit BF is different from the way it is done in the receive side. There are mainly two approaches to acquire these information at the transmit side [29]. In the first approach, the receiver estimates the CSI and sends it back to the transmitter via a feedback channel. This approach requires significant overhead in order to guarantee the accurate CSI at the transmitter, thus resulting in low spectral efficiency. The second approach is based on the channel reciprocity principle for time division duplex systems. This approach uses reverse CSI instead of the forward CSI in order to carry our transmit BF assuming channel reciprocity principle holds. Although this holds in the propagation channel if the time interval between uplink and downlink is less than the channel coherence time, this may not be true for the effective channel since it also consists of RF paths at the transmitter and receiver and transmit and receive RF chains for each antenna may be different. One solution to address this channel non-reciprocity is to apply a proper calibration method in order to compensate the difference between uplink and downlink [29].

In this work, a raster scan based approach is followed in acquiring the DoAs of the interfering FSS stations in the forward link scenario. In the return link, we employ blind and sector-based approaches, which do not need the exact knowledge about the locations of victim stations. In the following, we briefly describe the steps followed in the employed DoA estimation method considering antenna structure with 8 auxiliary elements on the top of the reflector, and then discuss the associated challenges.

1. Using the data available under ASPIM project [26], for each FSS terminal, three stronger interfering links were found and their corresponding positions were extracted.

2. The desired direction was set at $\theta = 149.4665°$, $\phi = 107.3942\circ$ corresponding to the pointing direction of the FSS terminal, elevation $=29°$ and azimuth $=190°$.

3. The nearest angular values (θ and ϕ), corresponding to the desired direction mentioned in step (2) and the interfering directions noted in step (1), in $theta \in [0\ 180]$ degree with the spacing of 0.1 degree and $\phi \in [0^\circ\ 360^\circ]$ with the spacing of 1 degree were computed.

4. Using the patterns of 8 auxiliary radiators, 1×8 array steering vector in the desired direction and a 3×8 array steering matrix in the directions of three interfering FS stations are computed.

5. By using the SNR, and INR values obtained from the considered interference scenario and the array steering vectors towards the desired and interfering links, covariance matrix R was computed.

6. Then, the raster scan method was employed to estimate the power spectrum using the following procedure.

   (a) The grids for the raster scan were considered same as per θ and ϕ spacings, i.e., 361 for $\phi \in [0^\circ\ 360^\circ]$ and 1801 for $\phi \in [0^\circ\ 360^\circ]$.

   (b) For each $\theta - \phi$ grid point, a steering vector $\mathbf{a}(\theta, \phi)$ was computed and was normalized with its maximum value in order not to alter the computed power levels with its amplitude.

   (c) Then the following expression (Bartlett Beamformer) was applied to capture the received power from the considered (θ, ϕ) direction

$$P(\theta, \phi) = \mathbf{a}^\dagger(\theta, \phi)\mathbf{R}\mathbf{a}(\theta, \phi), \tag{3}$$

   where $\mathbf{R}$ is computed using the following equation

$$\mathbf{R} = \sigma_d^2 \mathbf{a}(\theta_d, \phi_d)\mathbf{a}^\dagger(\theta_d, \phi_d) + \sum_{k=1}^{K} \sigma_k^2 \mathbf{a}(\theta_k, \phi_k)\mathbf{a}^\dagger(\theta_k, \phi_k) + \sigma_z^2 \mathbf{I}, \tag{4}$$

   where σ_d^2, σ_k^2 and σ_z^2 denote the power levels of the desired signal, interfering signal and the noise.

   (d) Steps (b) and (c) were repeated for all possible (θ, ϕ) within the defined ranges. The power spectrum obtained using the above steps was then normalized with its maximum value, which is shown in Figure 4.

7. The next step is to estimate the peaks from the power spectrum obtained using raster scan approach. This was carried out using the peak detection based on the predefined window in the following way.

   (a) By using the known desired direction, an area from the considered 2D image was eliminated around the desired direction with an window size of 10×10 degrees in both θ and ϕ planes (this corresponds to the the mainlobe width of the benchmark structure). This was done not to degrade the peak directivity by eliminating the cases where DoA estimator may estimate the angles close to the boresight direction.

   (b) Then the peak detection algorithm was applied in the 2D image obtained using step (a). First, the maximum value over the 2D grid is calculated and then a window size of 25×40 degrees in ϕ and θ planes around the maximum value is eliminated. In the ideal case, this size can be chosen in order to match with the null width of the pattern.

   (c) Subsequently, the maximum value over the 2D image obtained from step (b) is calculated, and then a window size of 25×40 degrees in ϕ and θ planes around the maximum value is eliminated.

   (d) Step (c) is repeated for estimating another interfering point and three stronger interfering directions are estimated in this way.

Figure 4 presents the power specturm plot obtained from the raster scan method along with the desired, true and estimated interfering directions. In the evaluated case, the strengths of the interfering signals were found to be $[50.8811^\circ \ -42.9704^\circ \ -48.5628^\circ]$ dBW considering the typical noise power of -126 dBW over 62.5 MHz carrier bandwidth). For the considered FSS terminal, the estimated interfering directions using the aforementioned estimation method were found at $\theta = [110.2^\circ \ 108.5^\circ \ 111.10^\circ]$ and $\phi = [0^\circ \ 340^\circ \ 21^\circ]$, whereas the true interfering directions for the considered case correspond to $\theta = [110.2346^\circ \ 16.1215^\circ \ 15.9044^\circ]$ and $\phi = [0.0615^\circ \ 180.1168^\circ \ 359.7863^\circ]$. It is clear that the employed estimator detects the strongest interfering direction correctly but detects other interferers in its vicinity since the first interfering link is very much stronger than other interfering links.

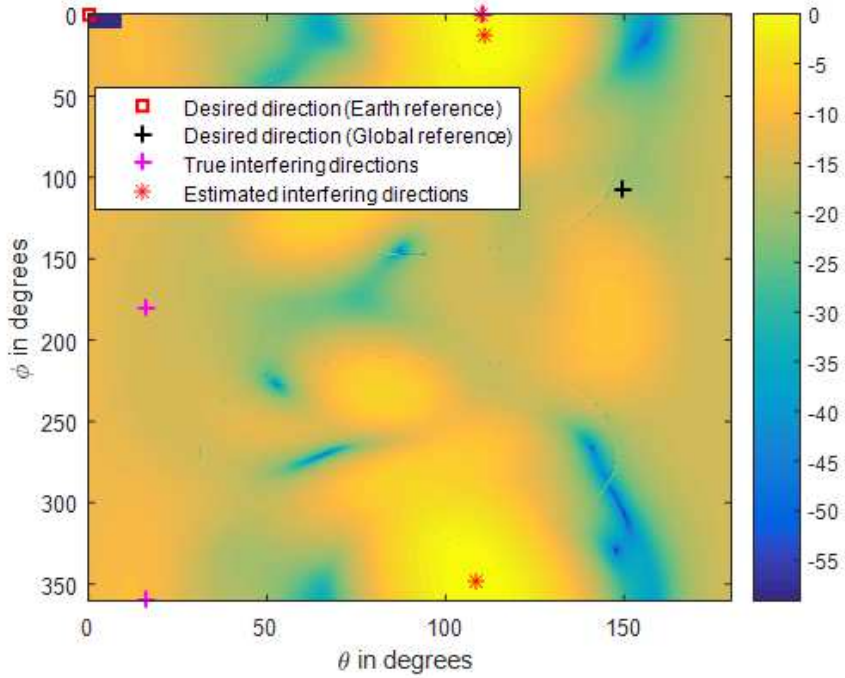

Figure 4: Illustration of power spectrum plot from raster scan (desired, true and estimated interfering directions are indicated in the plot, the colorbar shows the relative power levels in dB)

From the numerical analysis, it has been observed that the performance of the DoA estimator depends on the range of the interference power as well as the angular separation between interfering locations. If one of the interference power levels is very strong compared to other interference power levels, the interfering power lobe becomes so large that the algorithm detects 2nd and 3rd highest interfering locations in the same lobe even if the window size is considered significantly large. The important point here is that the strongest interfering direction is estimated with very good accuracy and the nulling algorithm will put nulls in this strongest direction as well as in the estimated interfering directions which are closer to this strongest interfering direction.

VI. Sidelobe Suppression

SL suppression at the FSS terminal using the considered antenna structure (array of auxiliary elements on the top of the main reflector) can be carried by employing either single stage joint processing or two-stage signal processing. In the single stage joint processing, antenna patterns of all auxiliary radiators and the main radiator are processed jointly. Whereas in the two-stage processing, first, a combined auxiliary pattern is generated by applying a suitable signal processing algorithm to the patterns of auxiliary radiators, and then the combined auxiliary pattern is mixed

with the main pattern by adjusting proper weighting coefficients in order to get the final pattern. In this paper, we base our analysis on the second approach. For our analysis, high interference scenario (in terms of the number of FS stations) in Poland is considered for the forward link and high interference scenario in Slovakia is considered for the return link.

In the forward link, two-stage SL suppression approach was followed to create nulling towards three stronger interfering directions. In the first stage, three sets of BF coefficients were designed in order to steer the auxiliary beam patterns in the directions of the three interfering FS stations (with raster scan based estimation, the interfering directions were found at $\theta = [110.2^\circ\ 108.5^\circ\ 111.1^\circ$ degrees and $\phi = [0^\circ\ 340^\circ\ 21^\circ]$) degrees, creating three steered auxiliary combined beam patterns. To create these auxiliary beampatterns, steering vector approach was followed, i.e., to generate an kth auxiliary beampattern steered towards kth interfering direction, the weighting coefficients were calculated using the following equation

$$\mathbf{w}_k = \mathbf{a}^\dagger(\theta_k, \phi_k), \tag{5}$$

where $\mathbf{a}(\theta_k, \phi_k)$ is the array response vector in the kth interfering direction.

Subsequently, using three auxiliary combined patterns generated in the first stage and the main feed pattern, Linearly Constrained Minimum Variance (LCMV) approach was followed in order to generate the final beampattern. The optimization problem for the LCMV beamformer can be written as [30]

$$\begin{aligned} &\min_{\mathbf{w}} \mathbf{w}^\dagger \mathbf{R} \mathbf{w}, \\ \text{subject to } &\mathbf{w}^\dagger \mathbf{a}(\phi_d, \theta_d) = 1, \\ &\mathbf{C}^\dagger \mathbf{w} = \mathbf{f}, \end{aligned} \tag{6}$$

where $\mathbf{C}$ is an $N \times (K+1)$ constraint matrix, $\mathbf{f}$ is an $(K+1) \times 1$ response vector, $\mathbf{R}$ is the covariance matrix computed using the response vectors derived from three auxiliary patterns generated in the first stage and the main The solution of (7) is given by

$$\mathbf{w} = \mathbf{R}^{-1}\mathbf{C}(\mathbf{C}^\dagger \mathbf{R}^{-1} \mathbf{C})^{-1}\mathbf{f}. \tag{7}$$

The above equation was evaluated using $\mathbf{f} = [1, \epsilon, ..., \epsilon]$ with ϵ being the response constraint in the interfering direction. As an example of our results, we present the 3D copolar pattern and 2D cut of the copolar pattern in Figure 5 considering a fixed FSS terminal in the worst case condition, i.e., the terminal receiving the highest aggregated interference in the considered high interference scenario of Poland.

In the return link, statistical analysis was carried by considering a single FS station (which receives the highest aggregated interference) in the high interference scenario of Slovakia. From the signal analysis point of view, both sector-based and blind approaches were employed. In the first approach, a single stage LCMV was used assuming the prior knowledge of the victim sector whereas in the second approach, a single stage Minimum Variance Distortionless Response (MVDR) beamformer considering the main beam pattern and all auxiliary patterns. The sector based approach was applied by putting multiple nulling constraints in (7) as in [8].

The optimization problem for MVDR approach is given by

$$\begin{aligned} &\min_{\mathbf{w}} \mathbf{w}^\dagger \mathbf{R} \mathbf{w} \\ \text{subject to } &\mathbf{w}^\dagger \mathbf{a}(\phi_d, \theta_d) = 1. \end{aligned} \tag{8}$$

The solution of above optimization problem is given by;

$$\mathbf{w} = \frac{\mathbf{R}^{-1}\mathbf{a}(\theta_d, \phi_d)}{\mathbf{a}^\dagger(\theta_d, \phi_d)\mathbf{R}^{-1}\mathbf{a}(\theta_d, \phi_d)}. \tag{9}$$

In contrast to the LCMV approach, MVDR beamformer does not need to know the location of the interfering FS stations.

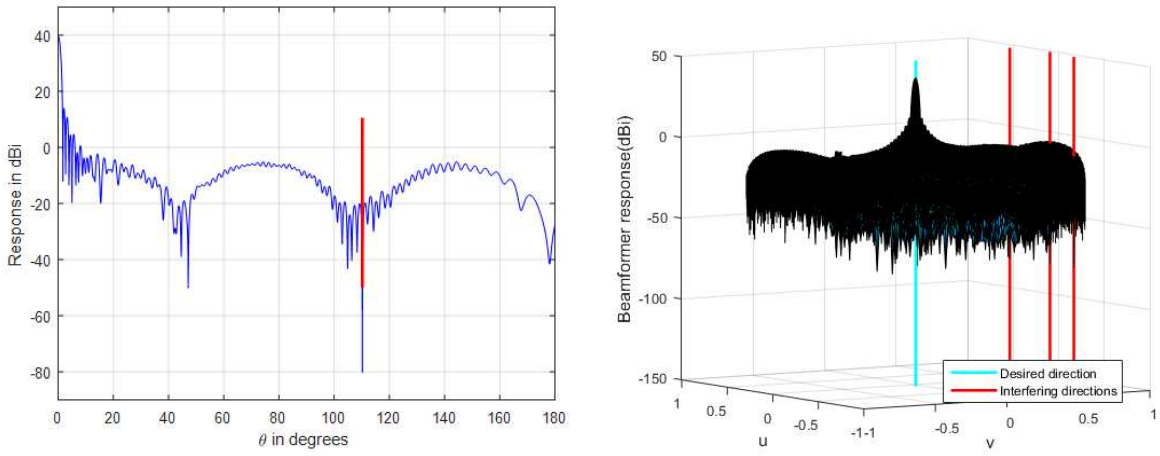

(a) (b)

Figure 5: 3D final copolar beam pattern after employing two-stage SL suppression with three estimated interfering directions, $\epsilon = 0.000001$

In Figures 6 (a) and 6 (b), we present the CDF plots of interference levels using sector based and blind approaches, respectively. From the presented plots, it can be noted that sector based approach provides no harmful interference at the FS stations (considering the interference threshold of -136 dBW) but the blind approach may create harmful interference at the FS receiver for some of the cases. However, average peak directivity with the blind approach was found to be higher than with the blind approach.

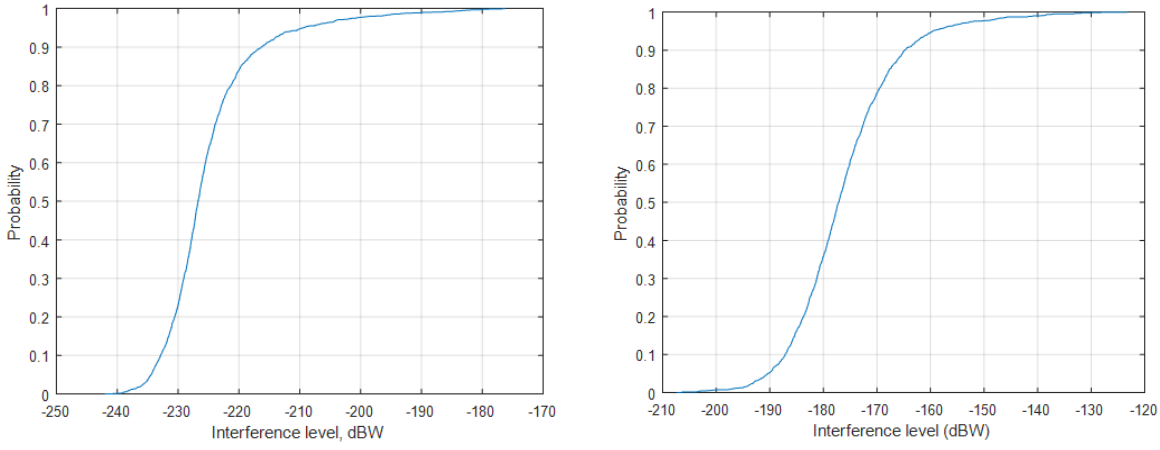

(a) (b)

Figure 6: CDF plot of interference level in the return link scenario with SLS configuration (a) using sector-based approach, (b) blind approach

VII. Beamforming

Herein, we consider the FAR antenna configuration having a parabolic reflector with a cluster of 7 feeds. In the forward link, the performance was analysed considering the high interference scenario of Poland as in the SLS case. We apply Capon (MVDR) beamformer as described in the previous subsection. In order to generate the evaluation scenario, three stronger interferers located

at $\theta = [110.2346^\circ\ 16.1215^\circ\ 15.9044^\circ]$ and $\phi = [0.0615^\circ\ 180.1168^\circ\ 359.7863^\circ]$ in the considered scenario were considered and the desired FSS satellite direction at $\theta = 0$ degree and $\phi = 0$ degree. In Figures 7 (a) and 7 (b), we present the 2D cuts of copolar pattern at $\phi = 0$ degree, and $\phi = 180$ degree, respectively. From the presented results, the nulls created in three interfering directions were about -40 dB in the first interfering direction, about -47 dB in the 2nd interfering direction and about -27 dB in the third interfering direction.

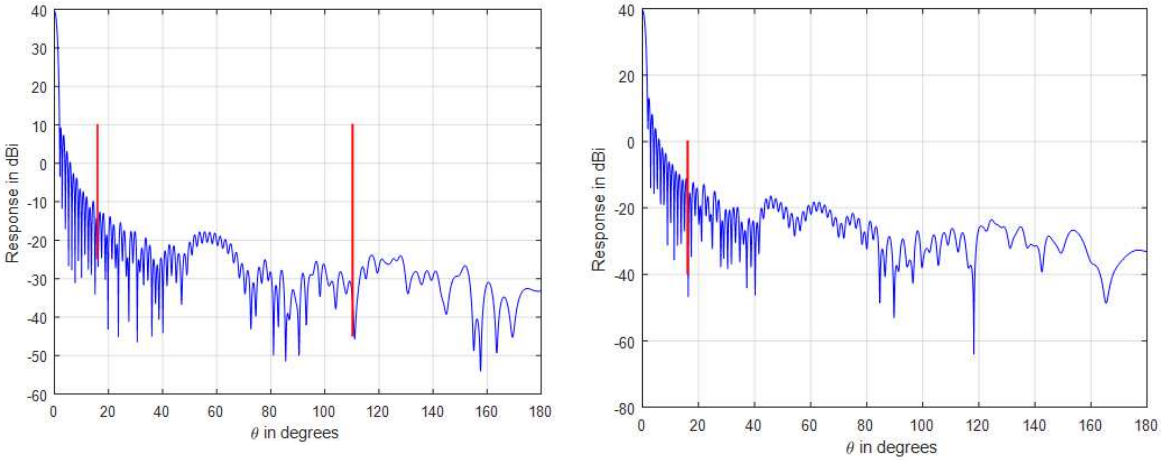

(a) (b)

Figure 7: 2D cut of the copolar pattern at (a) $\phi = 0$ degree, (b) $\phi = 180$ degree

In the return link, both blind and sector based approaches were analyzed in the high interference scenario of Slovakia with the same settings as described for the SLS case. In Figures 8 (a) and 8 (b), we present the CDF plots of interference levels using sector-based and blind approach obtained using the statistical analysis over 2000 FS stations, respectively. While comparing the presented results, it can be noted that the there exist some interference situations with the blind approach, however, all the interference situations are resolved in the sector based approach.

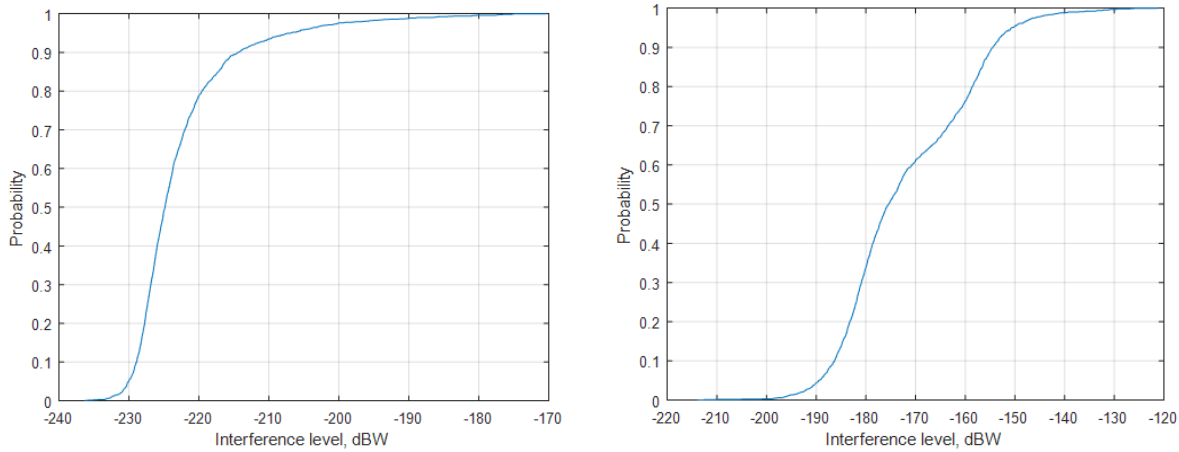

(a) (b)

Figure 8: CDF plot of interference level in the return link scenario with FAR configuration (a) using sector-based approach, (b) blind approach

VIII. Practical Considerations

It should be noted that the implementation of a BF technique requires a significant upgrade in the existing FSS system. In the terminal-side BF, a major upgrade in the terminal side is needed since a terminal equipped with multiple antennas is required to create a desired beam pattern. In spite of these required upgrades, it is still important to explore the application of the terminal-side BF in the next generation satellite systems in order to enhance the spectral efficiency of future satellite systems. In the following, we describe several practical aspects related to terminal-side BF.

1. **Terminal/System Cost**: The user terminal is a very cost sensitive element and its cost may significantly affect the success of any technology. The beamformer's cost is one of the main contributors to the user terminal cost. Therefore, the cost of the beamforming module should be minimized in order to increase its market acceptability/popularity. Recent advances in Monolithic Microwave Integrated Circuit (MMIC) technology, digital signal processing techniques/algorithms have made this technology cheaper and will become affordable for FSS users in the near future [31]. One possible way for reducing the implementation cost in the system level is to employ BF technique only in those FSS terminals which receive/cause harmful interference. This can be realized by setting a suitable SINR threshold determined based on the ModCod degradation of the terminal and then employing BF in that terminal whose SINR value is less than a certain threshold. From the system's perspective, it is an important aspect to identify which terminals are in the bad SINR conditions beforehand in order to implement this approach. In order to facilitate this, extensive link level and interference analysis may be carried out over the area of interest.

2. **Forward link versus Return link**: Due to the presence of multipath effects which are frequency selective, the forward channel and the return channel for an FSS terminal are not reciprocal in practice. This leads to the DoA acquisition problem difficult in forward and return links. Implementing transmit BF in the uplink scenario is more challenging since the terminal is transmitting and also it has to perfectly protect the incumbent FS receivers. However, since the transmit power in the uplink is low and directions of FSS and FS transmissions are highly directive in different planes, the interference may not be harmful in most of the cases. Depending on the terrain height and the height of terminals, there might be a few cases in which an FS receiver receives severe aggregate interference from the FSS transmissions. As an example, from the interference analysis carried out for Slovenia in CoRaSat project [32] by using FS database extracted from the TU-R BR International Frequency Information Circular (BR IFIC, the aggregate interference generated by the FSS system exceeds the acceptable interference threshold (-137.55 dBW@7 MHz) at the FS station for only less than 5 % of the cases.

   However, from the regulation perspective, interference above interference threshold limit is not allowed even for a small number of cases or for the small percentage of the time. While employing BF algorithms in this coexistence scenario, in practice, it may happen that some FS receivers which are located in the worst places (due to their geographical placements) may receive strong interference from the FS stations even if we employ BF techniques to mitigate interference towards a limited sector. Besides, it may not be possible to find the exact geographical location of the sector which can be generalized for all the possible FSS positions within the considered area of deployment.

3. **Elevation angle as an additional degree of freedom**: In the considered coexistence scenario, the elevation angle can be utilized as an additional degree of freedom in designing the terminal-based BF. In general, FS transmissions are highly directive in the Earths horizontal plane and the GEO FSS transmissions are also directive but in different directions which depend on the elevation angle of the terminal with respect to the satellite. Range aware BF based on the above difference in the transmission characteristic of GEO FSS transmissions seems a promising approach. In this approach, the satellite terminals do not need to know the exact locations of the interfering/victim FS stations. If the FS stations are close to each

other, they can also be grouped together into a cluster and design a beamformer in order to mitigate interference towards/from a specified cluster. Furthermore, in the considered coexistence scenario, terminals elevation angle also needs to be account in order to properly take account of the actual interfering directions in the 3D space as evaluated in this work.

IX. Conclusions

One promising way to address the spectrum scarcity problem in SatCom systems is to exploit the use of non-exclusive Ka-band. In this regard, this paper considered the spectral coexistence of primary FS links with the secondary FSS systems in both downlink and uplink. A detailed review of the existing sidelobe suppression, beamforming techniques and the status of Ka-band terminal has been provided. Furthermore, the employed raster-scan based DoA estimation method has been described in detail. Moreover, the performance evaluation of one SLS and one BF configurations has been provided along with some numerical results. It can be concluded that the proposed signal processing techniques are capable of performing nulls in the interfering directions while maintaining the sufficient boresight gain in the considered coexistence scenarios. From the practical perspectives, implementing transmit beamforming in return link scenario is more challenging than employing the receive beamforming in the forward link scenario.

Acknowledgement

This work was supported by the European Space Agency (ESA) project ASPIM "Antennas and Signal Processing Techniques for Interference Mitigation in Next Generation Ka Band High Throughput Satellites" (ESTEC Contract No. 4000111686/14/NL/FE). We would like to acknowledge Space Engineering, Italy and VTT, Finland for providing data for the performance evaluation during ASPIM project. The views presented in this paper are those of the authors and do not in any way represent the views of ESA.

References

[1]P. Chini, G. Giambene, and S. Kota, "A survey on mobile satellite systems," *Int. J. Satell. Commun. Network*, vol. 28, no. 1, pp. 2957, 2009.

[2]S. K. Sharma, S. Chatzinotas, and B. Ottersten, "Satellite cognitive communications: Interference modeling and techniques selection," in *Proc. 6th ASMS and 12th SPSC*, Sept. 2012, pp. 111-118.

[3]Shree K. Sharma, S. Chatzinotas, B. Ottersten, "Cognitive Radio Techniques for Satellite Communication Systems", in *proc. IEEE VTC-fall*, Las Vegas, Nevada, Sept. 2013, pp. 1-5.

[4]S. Kandeepan, L. De Nardis, M.-G. Di Benedetto, A. Guidotti, and G. Corazza, "Cognitive satellite terrestrial radios," in *IEEE GLOBECOM*, Dec. 2010, pp. 1 –6.

[5]K. Liolis *et al.*, "Cognitive radio scenarios for satellite communications: The CoRaSat approach," in *FUNMS*, July 2013, pp. 1–10.

[6]W. Tang, P. Thompson, B. Evans, "Frequency Sharing between Satellite and Terrestral Systems in the Ka Band: A Database Approach", *IEEE Int. Conf. Communications (ICC)*, London, UK, Jun 2015.

[7]E. Lagunas, S. K. Sharma, S. Maleki, S. Chatzinotas, and B. Ottersten, "Resource Allocation for Cognitive Satellite Communications with Incumbent Terrestrial Networks", *IEEE Trans. on Cognitive Communications and Networking*, Nov. 2015.

[8]S. K. Sharma, S. Chatzinotas, J. Grotz, and B. Ottersten, "3D Beamforming for Spectral Coexistence of Satellite and Terrestrial Networks", in *Proc. IEEE VTC-fall*, Sept. 2015.

[9]S. K. Sharma *et al.*, "Joint carrier allocation and beamforming for cognitive SatComs in Ka-band (17.3-18.1 GHz)," in *Proc. IEEE ICC*, June 2015.

[10]H. L. Van Trees, "Optimum Array Processing: Detection, Estimation and Modulation Theory", Part IV, Wiley, 2002.

[11]United States Patent 4,376,940, "Antenna arrangements for suppressing selected sidelobes", H. Miedema, March 15, 1983.

[12]United States Patent 3815146, "Multiple feed for microwave parabolic antennas", Walter E. Buehler and et al, June 4, 1974.

[13]United States Patent 4571594, "Directional antenna system having sidelobe suppression", Randy L. Haupt, February 18, 1986.

[14]United States Patent, 4,631,547, "Reflector antenna having sidelobe suppression elements", Daniel Jacavanco,

December 23, 1986.
[15]United States Patent 4725847, "Reflector antenna having sidelobe nulling assembly with metallic gratings", J. Leon Poirier, February 16, 1988.
[16]Randy L. Haupt , "Adaptive nulling with a reflector antenna using movable scattering elements", *IEEE Transactions on Antennas and Propagation*, Volume: 53 , Issue: 2 , 2005 , Page(s): 887 890.
[17]S. K. Sharma, S. Chatzinotas, and B. Ottersten, "Cognitive Beamforming for Spectral Coexistence of Hybrid Satellite Systems", in *Co-operative and Cognitive Satellite Systems*, Elsevier, 2015
[18]A. Geise, and et al, "Smart Antenna Terminals for Broadband Mobile Satellite Communications at Ka-Band," *2nd International ITG Conference on Antennas*, pp. 199-204, 28-30 March 2007.
[19]L. Baggen, and et al, "Designing integrated frontends for SatCom applications," in *International Semiconductor Conference (CAS)*, vol.1, no., pp.11-18, 15-17 Oct. 2012.
[20]S. K. Sharma, S. Chatzinotas, and B. Ottersten, "Spatial filtering for underlay cognitive SatComs," in *Proc. 5th Int. Conf. PSATS*, June 2013.
[21]S. K. Sharma, S. Chatzinotas, and B. Ottersten, "Transmit beamforming for spectral coexistence of satellite and terrestrial networks" in *Proc. 8th Int. Conf. CROWNCOM*, July 2013, pp. 275-281.
[22]J.A. Encinar, and M. Barba, "Reflectarray for K/Ka-band terminal antenna", available online: http://oa.upm.es/4496/2/INVE$_M EM_2008_61007.pdf$.
[23]J.-M. Baracco; P. Ratajczak, P. Brachat, and G. Toso, "Dual frequency Ka-band reflectarray for ground terminal application," 8th European Conference on Antennas and Propagation (EuCAP), pp. 1437-1440, 6-11 April 2014.
[24]Ruyuan Deng; Fan Yang; Shenheng Xu; Pirinoli, P., "Terahertz reflectarray antennas: An overview of the state-of-the-art technology," Electromagnetics in Advanced Applications (ICEAA), 2014 International Conference on , vol., no., pp.667-670, 3-8 Aug. 2014.
[25]J. Grotz, B. Ottersten, and J. Krause, "Signal detection and synchronization for interference overloaded satellite broadcast reception," IEEE Trans. Wireless Commun., vol. 9, no. 10, pp. 3052 3063, Oct. 2010.
[26]ESA ASPIM, "Antennas and Signal Processing Techniques for Interference Mitigation in Next Generation Ka Band High Throughput Satellites", ESA ESTEC Contract No. 4000111686/14/NL/FE.
[27]GRASP, http://www.ticra.com/products/software/grasp, 2000
[28]Barabell, "Improving the resolution performance of eigenstructure-based direction finding algorithms," in Proc. ICASSP83, Boston, MA, USA, April 1983, pp. 336-339.
[29]Chen Zhang, Jiqing Ni, Yantao Han, GaoKeDu, "Performance Analysis of Antenna Array Calibration and its Impact on Beamforming: A Survey", in Proc. 5th ICST conf. ChinaCom, Aug. 2010.
[30]R. Lorenz and S. Boyd, "Robust minimum variance beamforming," *IEEE Trans. Signal Process.*, vol. 53, no. 5, May 2005.
[31]P. K. Gupta and J. K. Hota, "Analysis of Low Cost Beamforming Techniques for LMS Communication Rx Terminal," International Conf. on Signal Processing and Communication, pp. 110 -114, 2013.
[32]CoRaSat project, Deliverable D3.4, "Comparative system evaluation and scenario-technique selection", available online: http://www.ict-corasat.eu/documents/deliverables.